ACES Asian Chemical Editorial Society

DOI: 10.1002/asia.201800498

CHEMISTRY AN ASIAN JOURNAL Full Paper

Reaction Mechanisms

SPECIAL ISSUE

Palladium-Catalyzed Divergent Arylation of Triazolopyridines: A Computational Study

Deyaa I. AbuSalim,[a] Sungwoo Hong,*[a, b] and Mu-Hyun Baik*[a, b]

Abstract: The mechanisms for new palladium-catalyzed divergent reactions of triazolopyridines were investigated by means of DFT calculations. Previously, it was observed experimentally that cross-coupling at the C7-position of triazolopyridines occurred when a strong base was used, whereas the reaction could be diverted to the C3-position if a weak base was employed. Calculations suggest that a strong base, such as *tert*-butoxide, can easily deprotonate C7–H, independent of the palladium metal, and deliver the preactivated substrate to palladium, which can reductively eliminate the final product. Without a strong base, the palladium(II) center reacts with the ring-opened diazo imine isomer of triazolopyridine to initially form a palladium(II)–carbene intermediate, which undergoes migratory insertion followed by β-hydride elimination to afford a 1,1-disubstituted alkene.

Introduction

Nitrogen-containing heterocycles are ubiquitous in biochemically and pharmaceutically important molecules, and are therefore important structural motifs to access many synthetic applications and have traditionally attracted much attention.[1] The 1,2,3-triazole moieties have been employed in many protocols to provide various useful synthetic transformations.[2] One interesting method, which has recently emerged as a particularly versatile general protocol for obtaining various N-heterocycles with precise regio- and stereocontrol, is based on 1,2,3-triazolepyridyl substrates that can liberate N_2 and produce various nitrogen-containing heterocycles.[3] Demonstrating the power of this methodology, we recently reported a palladium-catalyzed divergent arylation from triazolopyridines (Scheme 1).[4] This transformation relied on differentiation (C3 vs. C7) between the reactivity at the C7-position,[5] which was the most acidic site in the molecule, and the C3-position, which served as a carbene precursor. In addition, two concurrent arylation events were successfully performed in a one-pot process with a single palladium catalyst to afford 6-aryl-2-α-styrylpyridines of high synthetic utility. We concluded that the choice of base was important for obtaining high yields in these reactions. Interestingly, alkoxide bases (e.g., potassium *tert*-butoxide) favored reactivity at the C7-position, whereas carbonate bases (e.g., potassium carbonate) directed the reaction to the C3-position (Scheme 1). The mechanistic reason for the divergent behavior was not clear. Herein, we employed a DFT-based computational method to better understand these palladium-catalyzed reactions.

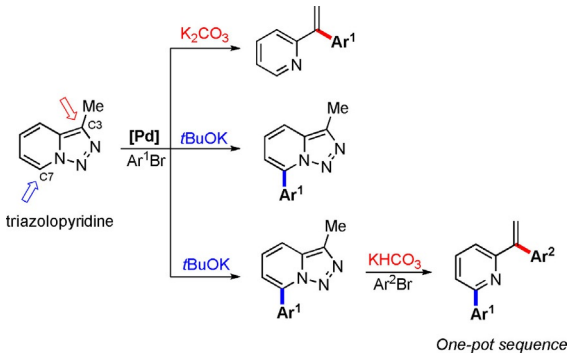

Scheme 1. Palladium-catalyzed divergent arylations of triazolopyridines.

Results and Discussion

After some exploratory calculations, we chose to construct a computational model system with tricyclohexylphosphine (PCy_3) as the supporting ligand on palladium in the reaction of triazolopyridine with bromobenzene, which was previously shown to afford effective arylation (Scheme 2). Cyclohexane rings on the PCy_3 ligand can adopt a multitude of conforma-

[a] D. I. AbuSalim, Prof. Dr. S. Hong, Prof. Dr. M.-H. Baik
Center for Catalytic Hydrocarbon Functionalizations
Institute for Basic Science (IBS)
Daejeon, 34141 (Republic of Korea)
E-mail: hongorg@kaist.ac.kr
mbaik2805@kaist.ac.kr

[b] Prof. Dr. S. Hong, Prof. Dr. M.-H. Baik
Department of Chemistry
Korea Advanced Institute of Science and Technology (KAIST)
Daejeon, 34141 (Republic of Korea)

Supporting information and the ORCID identification number(s) for the author(s) of this article can be found under:
https://doi.org/10.1002/asia.201800498.

This manuscript is part of a special issue on Homogeneous Catalysis from Young Investigators in Asia. Click here to see the Table of Contents of the special issue.

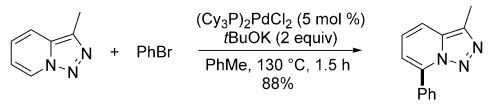

Scheme 2. C7 arylation of triazolopyridine with bromobenzene.

tions and relative orientations that may have an effect on their steric profile, based on intraligand, interligand, and anomeric effects.[6] A recent report by McMullin et al. analyzed the relative energies of these conformations and concluded that two orientations were most relevant.[6] We have considered several structural isomers and the most favored of these geometries has been employed in our study and used in all structures that include the PCy_3 moiety.

C7 Arylation

The proposed catalytic mechanism for arylation at the C7-position by using potassium butoxide as a base is shown in Figure 1, and the free energy profile is given in Figure 2. The reaction starts with an oxidative addition of bromobenzene to the resting state of the catalyst, bis(tricyclohexylphosphine)palladium(0) (**1**), which is calculated to have a barrier of $+26.4$ kcal mol^{-1} associated with transition-state **1-TS**, to form a *cis*-palladium(II) complex. Unsurprisingly, transition-state **1-TS** displays a three-center, four-electron interaction, which is characteristic of C–Br bond cleavage, accompanied by concerted metal–aryl and metal–Br bond formations, as shown in Figure 3a.[6,7] Although the immediate product of this oxidative addition step is the *cis*-palladium(II) complex, which was calculated at $+5.2$ kcal mol^{-1} (see the Supporting Information), it quickly isomerizes to give the corresponding *trans*-palladium(II)

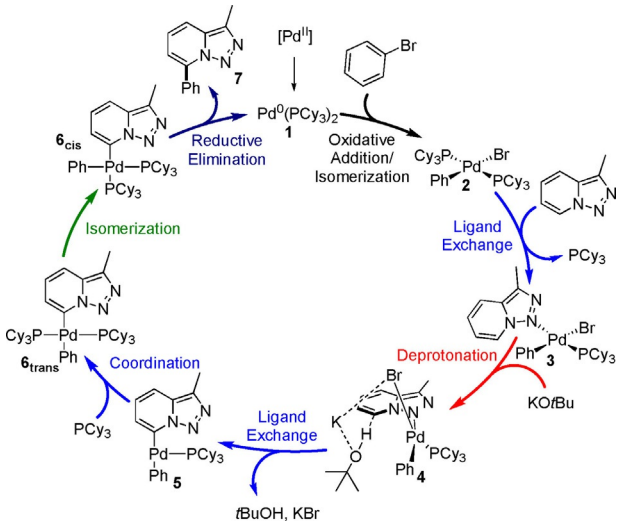

Figure 1. Proposed catalytic cycle for the C7 arylation of triazolopyridines with aryl bromides.

complex **2**, which has a relative free energy of -14.0 kcal mol^{-1}. Next, intermediate **2** can undergo ligand exchange to form a triazolopyridine palladium complex **3** at $+2.5$ kcal mol^{-1}, which facilitates a deprotonation of the C7–H, as illustrated in Figure 3b, with an activation energy barrier of -16.8 kcal mol^{-1} to form the transient high-energy intermediate complex **4**. Ligand exchange and extrusion of *tert*-butanol and KBr affords the coordinatively unsaturated intermediate **5**, which engages a free phosphine to give the palladium–aryl intermediate $\mathbf{6}_{trans}$ at -25.6 kcal mol^{-1}.

To facilitate the final C–C coupling, this intermediate must undergo a rearrangement to $\mathbf{6}_{cis}$ to place the two aryl ligands in *cis* disposition. Our calculations estimate this isomerization

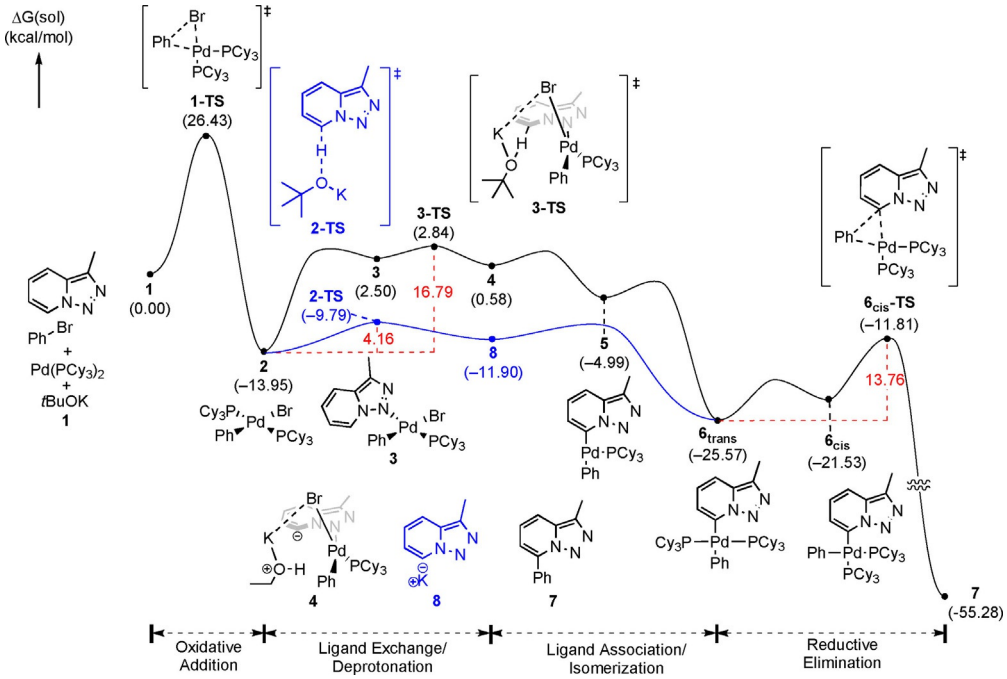

Figure 2. Computed free energy diagram for the two pathways investigated for C7 arylation.

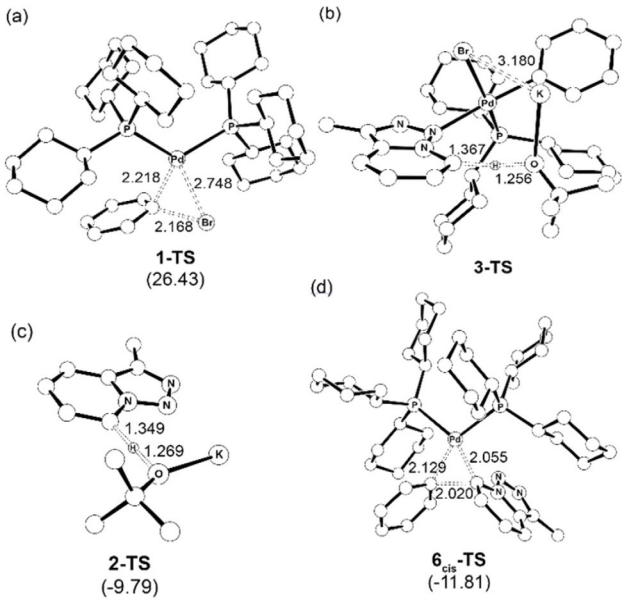

Figure 3. DFT-optimized geometries (bond lengths reported in Å) of a) **1-TS**, the three-centered oxidative addition of bromobenzene to palladium(0); b) transition state **3-TS**; c) transition state **2-TS**; and d) $\mathbf{6}_{cis}$**-TS**, the product forming three-centered reductive elimination. Nonessential hydrogen atoms are omitted for clarity and relative energies are given in kcal mol^{-1}.

to be viable at an energetic cost of only about 4 kcal mol^{-1}. Reductive elimination ensues, traversing transition-state $\mathbf{6}_{cis}$**-TS** to afford the final C–C coupled product with a barrier of +13.8 kcal mol^{-1}, as illustrated in Figure 2. The optimized structure is shown in Figure 3d and exhibits typical geometrical characteristics of reductive elimination with a C–C bond length of 2.02 Å.

Overall, the reaction is highly exergonic, with a total reaction free energy of −55.3 kcal mol^{-1}, and the most difficult step is the initial oxidative addition, with a computed barrier of 26.4 kcal mol^{-1}. Whereas the energies computed for the key steps of the mechanism are reasonable and show that the proposed mechanism is plausible, the deprotonation of the C7–H position is predicted to have a barrier of 16.8 kcal mol^{-1}, which is notably higher than that of the computed barrier of 13.8 kcal mol^{-1} for reductive elimination. Although it is not possible to reliably and quantitatively relate the computed barriers to reaction rates, because the pre-exponential collision factor in a standard Arrhenius-type equation cannot be determined, the energy differences are large enough that we can assign the oxidative addition step as being rate-determining in the reaction energy profile discussed above.

This finding is qualitatively consistent with the kinetic isotope effect (KIE) experiment reported previously, in which the k_H/k_D ratio of C7–H was found to be 1.1, which indicates that the deprotonation of C7–H is not involved in a turnover limiting step, as summarized in Scheme 3. However, given that the deprotonation step is calculated to be significantly higher than the reductive elimination step, one may anticipate a notable KIE. Thus, we reexamined the mechanism and considered an alternative pathway, in which deprotonation takes place prior to and separate from palladium interacting with the substrate.

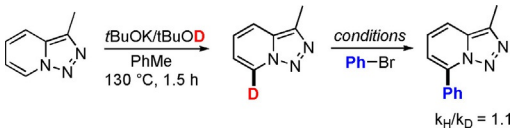

Scheme 3. KIE experiment for the C7 cross-coupling reaction.

In other words, the base attacks the C7–H moiety directly, which is plausible given the strong basicity of the *tert*-butoxide anion. This mechanistic pathway is also supported by the observation that full deprotonation of the substrate can occur in less than an hour in the absence of any palladium, as indicated in Scheme 2, and reported previously.[3] Of course, the fact that deprotonation can be observed does not mean that it has mechanistic value. In this regard, the DFT calculations presented herein are inspirational because experimental observations can be incorporated and unified into a quantitative and atomistic model of the mechanism.

Our calculations suggest that the simple acid/base reaction of the triazole substrate with potassium *tert*-butoxide traverses transition-state **2-TS** at +4.2 kcal mol^{-1} to readily afford potassium triazopyridyl salt **8** and *tert*-butanol at a relative free energy of −11.9 kcal mol^{-1}, as indicated in blue in Figure 2. Transmetalation with palladium complex **2** gives intermediate $\mathbf{6}_{trans}$, which may then continue on the same trajectory as that described above. This alternative low-energy pathway is also in good agreement with the deuterium labeling study summarized in Scheme 2. The extremely low barrier for deprotonation provides a convincing explanation for the observation that the KIE for the C7–H/D substrate was only 1.1. Thus, a slightly modified proposal for the mechanism is summarized in Figure 4.

C3 Arylation

It was observed during the experimental optimization of these reactions that the choice of base was critically important for the product distribution. Whereas strong alkoxide bases, for example, potassium *tert*-butoxide, favored the C7 arylation,

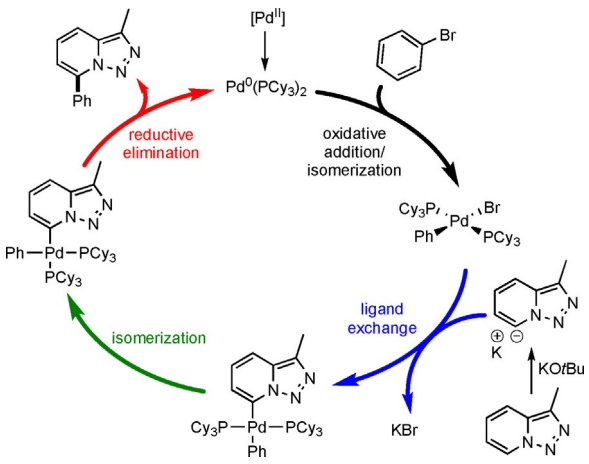

Figure 4. DFT-supported catalytic cycle for the C7 cross-coupling of triazolopyridines with aryl bromides.

weaker bases, such as potassium carbonate, gave C3 arylation products (Scheme 4). Given the functional role of *tert*-butoxide described above, a plausible explanation emerges that weak bases will be unable to deprotonate the substrate, which will result in a significant change to the reaction profile.

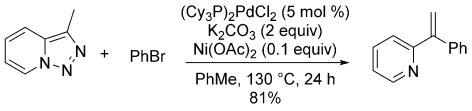

Scheme 4. C3 arylation of triazolopyridine with bromobenzene.

The most likely catalytic mechanism suggested by our calculations is shown in Figure 5 and the free energy profile is given in Figure 6. Of course, the initial oxidative addition to palladium(0) to form the *trans*-palladium(II) is identical to the reaction discussed above, but because there is no low-energy pathway to deprotonation followed by transmetalation, triazolopyridine $\mathbf{10_A}$ can isomerize to form the diazo imine $\mathbf{10_B}$, which is energetically uphill by $+5.5$ kcal mol^{-1}. Subsequent ligand exchange of $\mathbf{10_B}$ with the palladium(II) species raises the energy to $+3.1$ kcal mol^{-1} to form complex **11**. The loss of an equivalent of N_2 traversing the transition state **11-TS**, resulting in a barrier of 20.5 kcal mol^{-1}, affords palladium–carbene complex **12**. The computed structure of **11-TS** is illustrated in Figure 7a, and reveals a relatively late transition state with the C–(N_2) bond nearly cleaved at 1.84 Å and the triple-bond character between the two nitrogen atoms fully developed at a distance of 1.11 Å, which is very close to the N–N distance of about 1.10 Å found in free nitrogen gas. The liberation of N_2 has a decisive impact on the energy profile and intermediate **12** is found at a relative free energy of -22.9 kcal mol^{-1}, as illustrated in Figure 6.

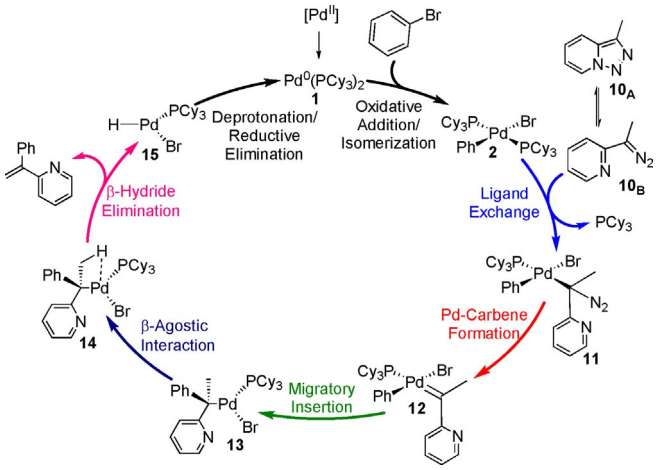

Figure 5. Proposed catalytic cycle for the C3 cross-coupling of triazolopyridines with aryl bromides.

Our calculations indicate that species **12** is not stable because migratory insertion of the carbene into the palladium–aryl bond has a very low barrier of only 3.3 kcal mol^{-1} and gives a new palladium(II) complex, **13**, which is located at -67.6 kcal mol^{-1}. The structure of transition-state **12-TS** is shown in Figure 7b and illustrates that the reason for its low energy is that insertion is assisted by the π orbitals of the aryl moiety and that of the carbene, which allows the C–C bond interaction to be relatively strong at a bond length of 2.48 Å, whereas the palladium–aryl bond is largely intact at 2.08 Å and so is the palladium–carbene bond at 1.95 Å. Newly formed intermediate **13** can undergo a slight structural distortion to iso-

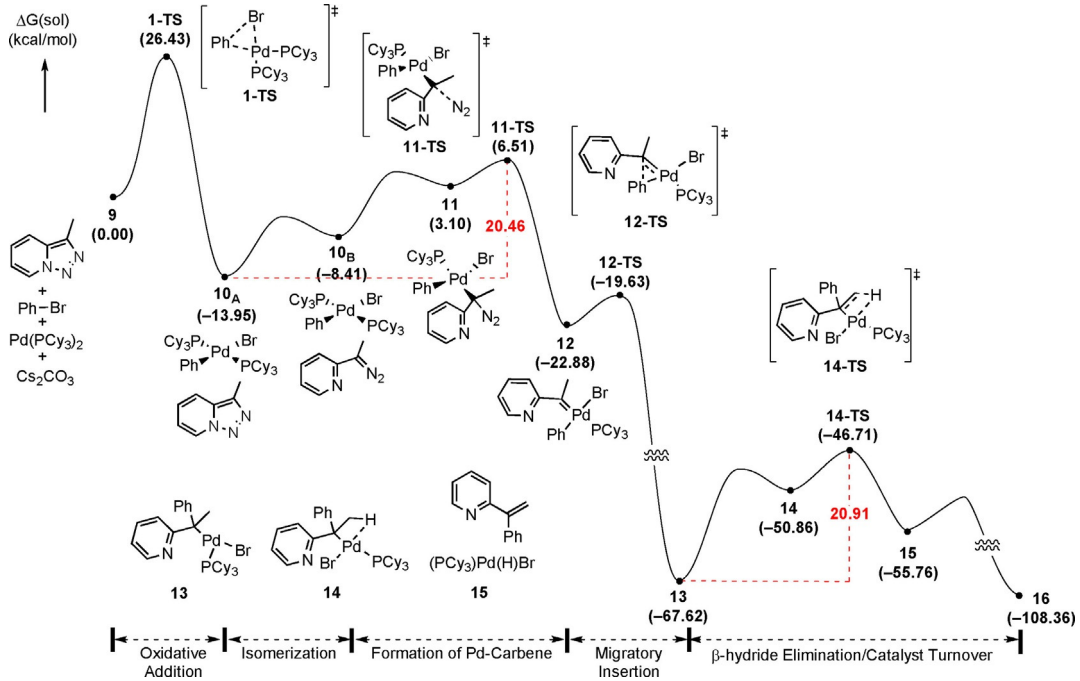

Figure 6. Computed free energy diagram for the C3 palladium–carbene reaction of triazolopyridines.

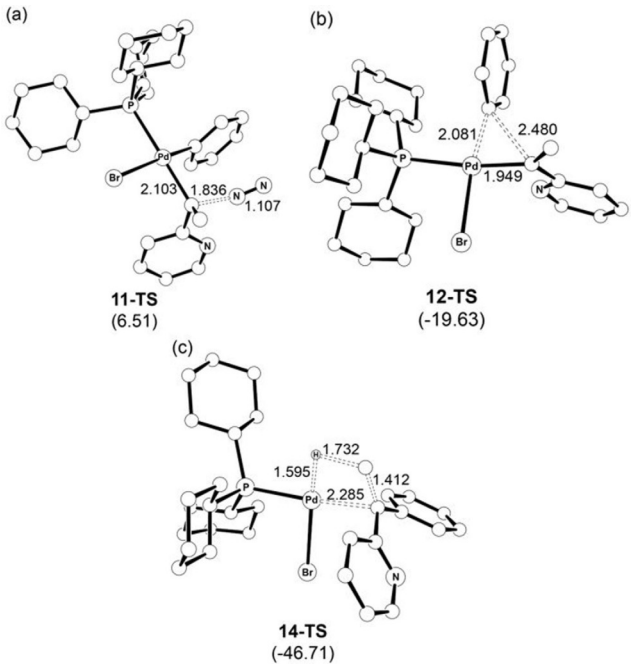

Figure 7. DFT-optimized geometries (bond lengths reported in Å) of a) transition-state **11-TS**, the transition state for N_2 loss; b) transition-state **12-TS**, the transition state for migratory insertion into the carbene; and c) transition-state **14-TS**, the transition state for β-hydride elimination. Nonessential hydrogen atoms are omitted for clarity and relative energies are given in kcal mol^{-1}.

merize to transient intermediate **14**, in which a β-H agostic interaction activates the C–H bond prior to undergoing β-hydride elimination. The barrier for this process associated with transition state **14-TS**, for which the Pd–H bond is calculated to be 1.60 Å (Figure 7c), was found to be +20.9 kcal mol^{-1}. The resulting palladium(II) hydride species **15**, which carries the final olefinic product, was located at −55.8 kcal mol^{-1}. To complete the reaction, species **15** reductively eliminates the product in the presence of a mild base, and ligand exchange of the bromide with a phosphine regenerates the palladium(0) catalyst. This step is highly exergonic by 52.6 kcal mol^{-1} to render the overall reaction to be downhill by 108.4 kcal mol^{-1}.

Conclusion

The mechanistic reason for the experimentally observed regiodivergent palladium-catalyzed arylation of triazolopyridine substrate at either the C3- or C7-positions was explored by means of DFT calculations. If a strong Brønsted base, such as *tert*-butoxide, was present, it would readily attack the hydrogen at the C7-position and deprotonate it without any involvement of the palladium catalyst. This process led to an arylic anion moiety that could be added to a palladium(II) intermediate through a simple transmetalation process. Because the palladium center already carried the other arylic coupling partner from the oxidative addition of an aryl halide in a previous step, standard reductive elimination might lead to the final C–C coupled product. In this case, the regiochemistry was predetermined by deprotonation. A weak base, on the other hand, could not deprotonate the triazolopyridine substrate directly, which effectively shut down the aforementioned simple pathway to the C–C coupled product. In such a case, the palladium metal engaged the open form of the triazolopyridine substrate and catalyzed the extrusion of N_2, leading to a palladium–carbene complex. Migratory insertion into the palladium–aryl bond and subsequent β-hydride elimination produced the disubstituted olefin product bound to the palladium–hydride complex. Finally, reductive elimination led to the release of the olefin and recovery of the palladium(0) catalyst. Here, the lack of a strong base forced the reaction to a route in which the key C–H activation step was accomplished by β-hydride elimination. The rate-determining step was predicted to be the initial oxidative addition of the aryl halide coupling partner to the palladium(0) catalyst.

Computational Details

All calculations were performed by using DFT, as implemented in the Jaguar 8.1 suite of ab initio quantum chemistry programs.[8] Geometry optimizations were performed with the M06 functional[9] by using the 6-31G** basis set. Pd and Br were represented by using the Los Alamos LACVP[10] basis set that included relativistic core potentials. More accurate single-point energies were computed from the optimized geometries by using Dunning's correlation-consistent triple-ζ basis set, cc-pVTZ(-f),[11] which included a double set of polarization functions. Pd and Br were represented by using a modified version of LACVP, designated as LACV3P, in which the exponents were decontracted to match the effective core potential with triple-ζ quality. Vibrational frequencies were computed at the M06/6-31G** level of theory to derive the zero-point energy (ZPE) and vibrational entropy corrections from unscaled frequencies. Entropy herein referred specifically to the vibrational/rotational/translational entropy of the solutes because the continuum model included the entropy of the solvent implicitly. All intermediates were confirmed as local minima on the potential energy surface with zero imaginary frequencies. Transition states were confirmed to possess only one imaginary frequency. Solvation energies were evaluated by using a self-consistent reaction field (SCRF)[12] approach based on accurate numerical solutions of the linearized Poisson–Boltzmann equation. Solvation calculations were carried out on the optimized gas-phase geometries by using a dielectric constant of $\varepsilon = 2.379$ for toluene. The change in solution-phase free energy, $\Delta G(\mathrm{sol})$, was calculated from Equations (1)–(5).

$$G(\mathrm{sol}) = G(\mathrm{gas}) + \Delta G(\mathrm{solv}) \quad (1)$$

$$G(\mathrm{gas}) = H(\mathrm{gas}) - \mathrm{TS}(\mathrm{gas}) \quad (2)$$

$$H(\mathrm{gas}) = E(\mathrm{SCF}) + \mathrm{ZPE} \quad (3)$$

$$\Delta E(\mathrm{SCF}) = \Sigma E(\mathrm{SCF})\ \text{for products} - \Sigma E(\mathrm{SCF})\ \text{for reactants} \quad (4)$$

$$\Delta G(\mathrm{sol}) = \Sigma G(\mathrm{sol})\ \text{for products} - \Sigma G(\mathrm{sol})\ \text{for reactants} \quad (5)$$

Acknowledgements

This research was supported financially by the Institute for Basic Science (IBS-R010-D1 and IBS-R010-G1). We sincerely

thank Dr. Daniel C. Ashley for his diligent training. We also thank Seihwan Ahn and Omaru M. Kabia for insightful conversations.

Conflict of interest

The authors declare no conflict of interest.

Keywords: arylation · carbenes · density functional calculations · palladium · reaction mechanisms

[1] a) G. Jones in *Comprehensive Heterocyclic Chemistry II, Vol. 5* (Eds.: A. R. Katritzky, C. W. Rees, E. F. V. Scriven, A. McKillop), Pergamon, Oxford, **1996**, p. 167; b) *Pharmaceutical Chemistry: Drug Synthesis, Vol. 1* (Eds.: H. J. Roth, A. Kleemann), Prentice Hall Europe, London, **1988**, p. 407; c) *Progress in Heterocyclic Chemistry* (Eds.: G. W. Gribble, J. A. Joule), Elsevier, Oxford, **2008**; d) N. K. Boaen, M. A. Hillmyer, *Chem. Soc. Rev.* **2005**, *34*, 267; e) A. G. Habeeb, P. N. P. Rao, E. E. Knaus, *J. Med. Chem.* **2001**, *44*, 3039; f) E. Vitaku, D. T. Smith, J. T. Njardarson, *J. Med. Chem.* **2014**, *57*, 10257.

[2] a) J. Wencel-Delord, F. Glorius, *Nat. Chem.* **2013**, *5*, 369; b) J. Yamaguchi, A. D. Yamaguchi, K. Itami, *Angew. Chem. Int. Ed.* **2012**, *51*, 8960; *Angew. Chem.* **2012**, *124*, 9092; c) S. H. Cho, J. Y. Kim, J. Kwak, S. Chang, *Chem. Soc. Rev.* **2011**, *40*, 5068; d) J. Wencel-Delord, T. Dröge, F. Liu, F. Glorius, *Chem. Soc. Rev.* **2011**, *40*, 4740; e) M. Schlosser, F. Mongin, *Chem. Soc. Rev.* **2007**, *36*, 1161; f) S. R. Chemler, P. H. Fuller, *Chem. Soc. Rev.* **2007**, *36*, 1153; g) B. Chattopadhyay, V. Gevorgyan, *Angew. Chem. Int. Ed.* **2012**, *51*, 862; *Angew. Chem.* **2012**, *124*, 886; h) H. M. L. Davies, J. S. Alford, *Chem. Soc. Rev.* **2014**, *43*, 5151; i) A. V. Gulevich, V. Gevorgyan, *Angew. Chem. Int. Ed.* **2013**, *52*, 1371; *Angew. Chem.* **2013**, *125*, 1411.

[3] a) N. Grimster, L. Zhang, V. V. Fokin, *J. Am. Chem. Soc.* **2010**, *132*, 2510; b) S. H. Cho, E. J. Yoo, I. Bae, S. Chang, *J. Am. Chem. Soc.* **2005**, *127*, 16046; c) I. Bae, H. Han, S. Chang, *J. Am. Chem. Soc.* **2005**, *127*, 2038; d) N. Selander, B. T. Worrell, V. V. Fokin, *Angew. Chem. Int. Ed.* **2012**, *51*, 13054; *Angew. Chem.* **2012**, *124*, 13231; e) T. Miura, Y. Funakoshi, M. Morimoto, T. Biyajima, M. Murakami, *J. Am. Chem. Soc.* **2012**, *134*, 17440; f) T. Miura, T. Biyajima, T. Fujii, M. Murakami, *J. Am. Chem. Soc.* **2012**, *134*, 194; g) N. Selander, B. T. Worrell, S. Chuprakov, S. Velaparthi, V. V. Fokin, *J. Am. Chem. Soc.* **2012**, *134*, 14670; h) M. Zibinsky, V. V. Fokin, *Angew. Chem. Int. Ed.* **2013**, *52*, 1507; *Angew. Chem.* **2013**, *125*, 1547; i) B. T. Parr, S. A. Green, H. M. L. Davies, *J. Am. Chem. Soc.* **2013**, *135*, 4716; j) J. E. Spangler, H. M. L. Davies, *J. Am. Chem. Soc.* **2013**, *135*, 6802; k) H. J. Jeon, D. J. Jung, J. H. Kim, Y. Kim, J. Bouffard, S.-G. Lee, *J. Org. Chem.* **2014**, *79*, 9865; l) D. J. Lee, H. S. Han, J. Shin, E. J. Yoo, *J. Am. Chem. Soc.* **2014**, *136*, 11606.

[4] Y. Moon, S. Kwon, D. Kang, H. Im, S. Hong, *Adv. Synth. Catal.* **2016**, *358*, 958.

[5] For other pyrozolo systems, see: a) K. H. Oh, S. M. Kim, M. J. Lee, J. K. Park, *Adv. Synth. Catal.* **2015**, *357*, 3927; b) R. B. Bedford, S. J. Durrant, M. Montgomery, *Angew. Chem. Int. Ed.* **2015**, *54*, 8787; *Angew. Chem.* **2015**, *127*, 8911.

[6] C. L. McMullin, N. Fey, J. N. Harvey, *Dalton Trans.* **2014**, *43*, 13545.

[7] a) E. Lyngvi, F. Schoenebeck, *Tetrahedron* **2013**, *69*, 5715; b) L. J. Goossen, D. Koley, H. L. Hermann, W. Thiel, *Organometallics* **2005**, *24*, 2398; c) A. Ariafard, Z. Lin, *Organometallics* **2006**, *25*, 4030; d) H. M. Senn, T. Ziegler, *Organometallics* **2004**, *23*, 2980; e) M. Ahlquist, P. Fristrup, D. Tanner, P.-O. Norrby, *Organometallics* **2006**, *25*, 2066.

[8] A. D. Bochevarov, E. Harder, T. F. Hughes, J. R. Greenwood, D. A. Braden, D. M. Philipp, D. Rinaldo, M. D. Halls, J. Zhang, R. A. Friesner, *Int. J. Quantum Chem.* **2013**, *113*, 2110.

[9] Y. Zhao, D. G. Truhlar, *Theor. Chem. Acc.* **2008**, *120*, 215.

[10] a) P. J. Hay, W. R. Wadt, *J. Chem. Phys.* **1985**, *82*, 270; b) P. J. Hay, W. R. Wadt, *J. Chem. Phys.* **1985**, *82*, 299.

[11] R. A. Kendall, T. H. Dunning, Jr., R. J. Harrison, *J. Chem. Phys.* **1992**, *96*, 6796.

[12] a) T. H. Dunning, Jr., *J. Chem. Phys.* **1989**, *90*, 1007; b) B. Marten, K. Kim, C. Cortis, R. A. Friesner, R. B. Murphy, M. N. Ringnalda, D. Sitkoff, B. Honig, *J. Phys. Chem.* **1996**, *100*, 11775; c) S. R. Edinger, C. Cortis, P. S. Shenkin, R. A. Friesner, *J. Phys. Chem. B* **1997**, *101*, 1190; d) M. Friedrichs, R. Zhou, S. R. Edinger, R. A. Friesner, *J. Phys. Chem. B* **1999**, *103*, 3057.

Manuscript received: April 2, 2018
Revised manuscript received: April 27, 2018
Accepted manuscript online: April 30, 2018
Version of record online: June 20, 2018